Surface-chemistry-driven actuation in nanoporous gold

J. Biener[1]*, A. Wittstock[1,2], L. A. Zepeda-Ruiz[1], M. M. Biener[1], V. Zielasek[2], D. Kramer[3], R. N. Viswanath[3], J. Weissmüller[3], M. Bäumer[2] and A. V. Hamza[1]

Although actuation in biological systems is exclusively powered by chemical energy, this concept has not been realized in man-made actuator technologies, as these rely on generating heat or electricity first[1]. Here, we demonstrate that surface-chemistry-driven actuation can be realized in high-surface-area materials such as nanoporous gold. For example, we achieve reversible strain amplitudes of the order of a few tenths of a per cent by alternating exposure of nanoporous Au to ozone and carbon monoxide. The effect can be explained by adsorbate-induced changes of the surface stress[2], and can be used to convert chemical energy directly into a mechanical response, thus opening the door to surface-chemistry-driven actuator and sensor technologies.

In the most general definition, an actuator is a device that converts some sort of energy into mechanical work. Exploring nanostructured high-surface-area materials for this purpose has recently attracted much interest[1,3,4]. Although most of the work in this field is focused on polymer- and carbon-nanotube-based materials[5], macroscopic and reversible strain effects have also been observed for nanoporous metals in an electrochemical environment[4,6]. In particular, nanoporous Pt and Au have been demonstrated to yield strain amplitudes comparable to those of commercial ferroelectric ceramics[4,6]. Although the microscopic processes behind the charge–strain response of nanoporous metals in an electrochemical environment are still under debate, it seems to be clear—in a continuum description—that the effect is caused by charge-induced changes in the surface stress f at the metal–electrolyte interface[7].
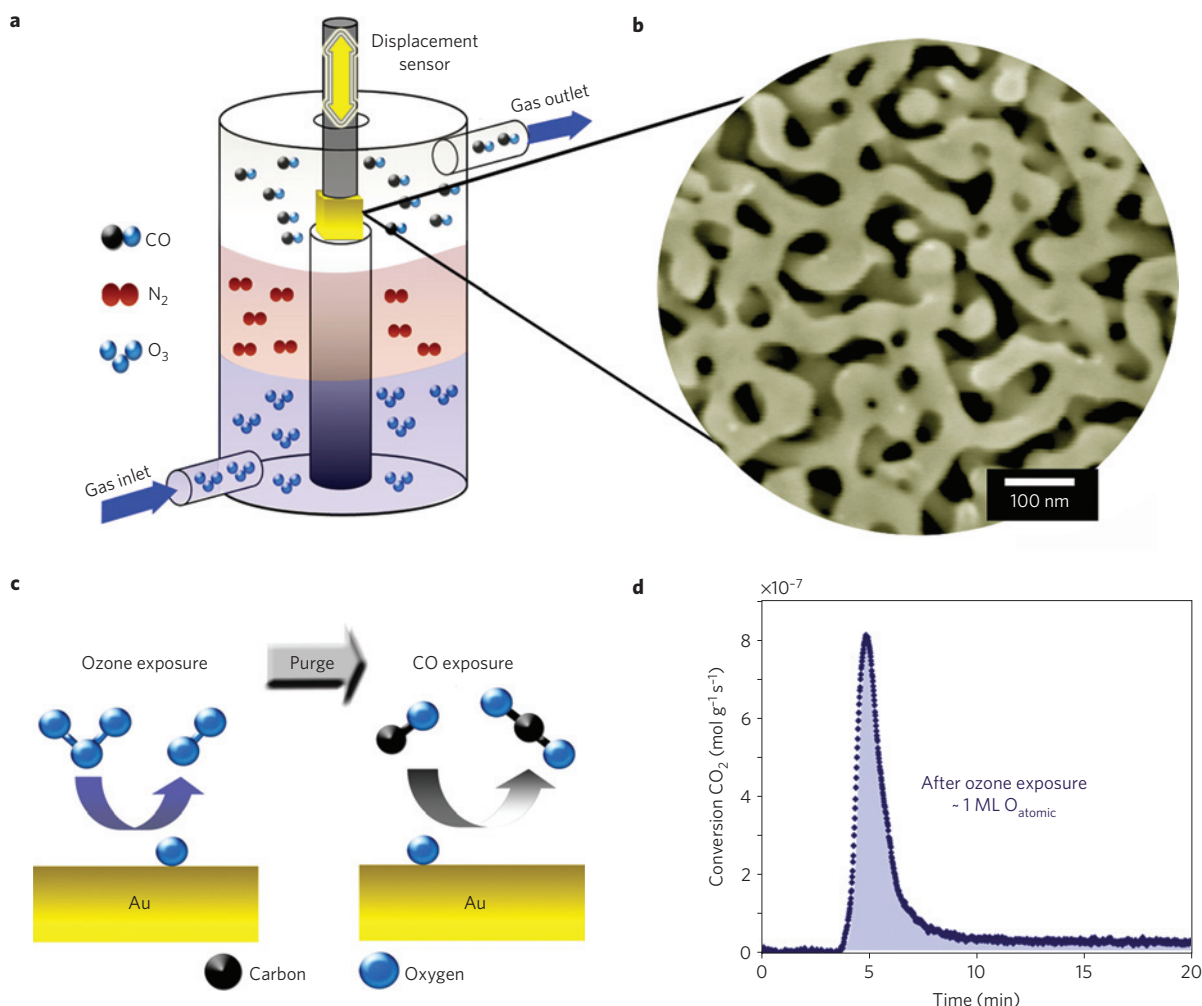
Here, we describe an actuator concept that is based on surface-chemistry-induced changes of the surface stress at a metal–gas interface, which, in turn, drives an elastic macroscopic sample contraction/expansion. This concept can be used to directly convert chemical energy into a mechanical response without generating heat or electricity first. The underlying principle, adsorbate-induced changes of the surface stress f of metal surfaces, has been the subject of intensive research[2,8]. Covalent adsorbate–metal interactions seem to have a decisive role in determining both the size and even the sign of adsorbate-induced changes of f (ref. 9). Although the relative change in f can be large, a macroscopic strain response can be achieved only by using high-surface-area materials. In the following, we report on *in situ* strain measurements on nanoporous gold. By using the oxidation of carbon monoxide by ozone, $CO + O_3 \rightarrow CO_2 + O_2$, as a driving reaction, we achieved reversible, macroscopic strains of up to 0.5%. Nanoporous Au is an ideal material for this experiment for several reasons. First and foremost, nanoporous Au exhibits unexpected catalytic properties. The material is reactive enough to catalyse surface reactions such as ozone dissociation[10] and CO oxidation[11,12] at room temperature, but it is also noble enough to prevent irreversible oxidation. Second, its characteristic sponge-like open-cell foam morphology[13] makes it a high-surface-area material that also combines high porosity (mass transport) with high strength (sustainable stress)[14]. Finally, ozone exposure can be expected to change the surface stress of Au as oxygen adsorption has been shown to cause a depletion of the Au $5d$ band[15].

Nanoporous Au can be easily prepared in the form of millimetre-sized monolithic samples by a process called 'dealloying'. In metallurgy, dealloying is defined as selective corrosion (removal) of the less noble constituent (here: Ag) from an alloy (Ag–Au), usually by dissolving this component in a corrosive environment[13,16]. In the case of Ag–Au alloys, this leads to the development of a three-dimensional bicontinuous nanoporous structure while maintaining the original shape of the alloy sample (see Fig. 1). The test specimens used here were prepared by dealloying 1 mm³ cubes of a $Ag_{75}Au_{25}$ master alloy in a standard three-electrode electrochemical set-up using a 1 M perchloric acid electrolyte[17]. The resulting Au foam samples had a porosity of $\sim 70\%$, and exhibit a specific surface area of ~ 10–$15\ m^2\ g^{-1}$ and a pore size of 10–20 nm. The strain measurements were carried out in a commercial dilatometer equipped with a sealed sample compartment for environmental control (Fig. 1a).

Typical macroscopic strain versus time data sets are shown in Fig. 2. Here, the strain was continuously monitored while the samples were alternately exposed to a mixture of 1–8% O_3 in O_2 and pure CO. Splitting the surface-catalysed oxidation of CO by O_3 into two self-limiting half-reactions enables us to switch the surface of nanoporous Au back and forth between an oxygen-covered and clean state (Fig. 1c): in the first half-cycle, ozone exposure leads to oxygen adsorption on the clean Au surface[10], $O_3 + Au \rightarrow Au-O + O_2$, whereas CO exposure in the second half-cycle restores the clean Au surface by reacting with adsorbed oxygen towards carbon dioxide[11], $CO + Au-O \rightarrow CO_2 + Au$. In contrast to oxygen, CO does not form a stable adsorbate layer on Au surfaces at room temperature, and the CO coverage will rapidly approach zero once the CO exposure is interrupted[18]. Details of the ozone–CO surface chemistry on nanoporous Au were studied by carrying out CO titration experiments in a continuous-flow reactor described in ref. 11. These experiments revealed that the oxygen saturation coverage that can be achieved on nanoporous Au by room-temperature

[1]Nanoscale Synthesis and Characterization Laboratory, Lawrence Livermore National Laboratory, Livermore, California 94550, USA, [2]Institut für Angewandte und Physikalische Chemie, Universität Bremen, 28359 Bremen, Germany, [3]Institut für Nanotechnologie, Forschungszentrum Karlsruhe, 76021 Karlsruhe, Germany. *e-mail: biener2@llnl.gov.

a

Displacement sensor

Gas outlet

CO

N₂

O₃

Gas inlet

b

100 nm

c

Ozone exposure — Purge → CO exposure

Au

Au

Carbon

Oxygen

d

×10⁻⁷

After ozone exposure ~ 1 ML O$_{atomic}$

Conversion CO₂ (mol g⁻¹ s⁻¹)

Time (min)

Figure 1 | Illustration of surface-chemistry-driven actuation in nanoporous gold. a, Nanoporous Au sample mounted in a viscous-flow reactor (residence time ~1 min). Adsorbate-induced dimensional changes of the nanoporous Au sample are measured by dilatometry. **b**, Scanning electron micrograph showing the characteristic sponge-like open-cell morphology of nanoporous Au. **c**, Au surfaces can be switched back and forth between an oxygen-covered and clean state by alternating exposure to ozone (O_3) and carbon monoxide (CO). **d**, CO titration experiment on nanoporous Au after ozone saturation exposure at room temperature. The integrated CO_2 signal intensity reveals an oxygen saturation coverage of approximately one monolayer (ML; $\sim 10^{15}$ cm^{-2}) in excellent agreement with ref. 10.

ozone exposure is approximately one monolayer, and that this chemically adsorbed oxygen can be readily removed by room-temperature CO exposure (Fig. 1d). Both observations are in excellent agreement with single-crystal experiments[10,12] and demonstrate that ozone-induced oxygen uptake is limited to a monolayer rather than fully oxidizing nanoporous Au.

The data shown in Fig. 2a reveal that O_3 exposure (chemisorption of oxygen) causes a sample contraction, whereas CO exposure restores the original sample dimensions by reacting with adsorbed oxygen. The strain amplitude increases with both cycle length (Fig. 2c) and the O_3 concentration (Fig. 2d), and typical strain values lie in the range from 0.05 to 0.5%. Note that a strain amplitude of 0.5% corresponds to a macroscopic actuator stroke of 5 μm for a 1-mm-long sample. A small irreversible component is superimposed on the elastic response, which becomes more pronounced for larger actuator strains. This might indicate plastic yielding or, more consistent with the slow kinetics, stress-driven diffusion creep.

Note that the contraction on ozone exposure can be observed only for Ag–Au samples dealloyed at potentials around 700 mV (measured against a Ag/AgCl reference electrode). In contrast, ozone exposure leads to expansion (with a similar amplitude) in

samples dealloyed at higher potentials. In general, the expansion could be the result of sample heating through exothermic surface reactions, but more studies will be necessary to understand the impact of the dealloying conditions on the effects described here.

Although we record only the uniaxial strain response $\Delta l/l$ of our system, it is truly a three-dimensional phenomenon, where in the limit of small strains, the volume change $\Delta V/V$ is given by $3 \Delta l/l$. As nanoporous Au can sustain macroscopic stresses of up to 200 MPa (ref. 19), the actuator concept described here has a $P\mathrm{d}V$ work density of ~ 3 MJ m^{-3}, which is comparable to that of a shape-memory-alloy-based system described recently by Ebron *et al.*[1]. The advantage of the surface-stress-driven actuator concept described here is that maintaining the strain does not require the continuous supply of chemical energy. The efficiency of the actuator can be estimated from the standard Gibbs energy of reaction of the CO oxidation by O_3 (~ 420 kJ mol^{-1}) and the number of surface atoms ($\sim 1{,}000$ mol m^{-3} for nanoporous Au with a specific surface area of ~ 10 m^2 g^{-1} and density of 6×10^6 g m^{-3}). Using the oxygen saturation coverage of approximately one monolayer ($\sim 10^{15}$ cm^{-2}) obtained from the CO titration experiment on nanoporous Au shown in Fig. 1d reveals an efficiency of the order of 1%. The low efficiency is a direct consequence of the strongly exothermic
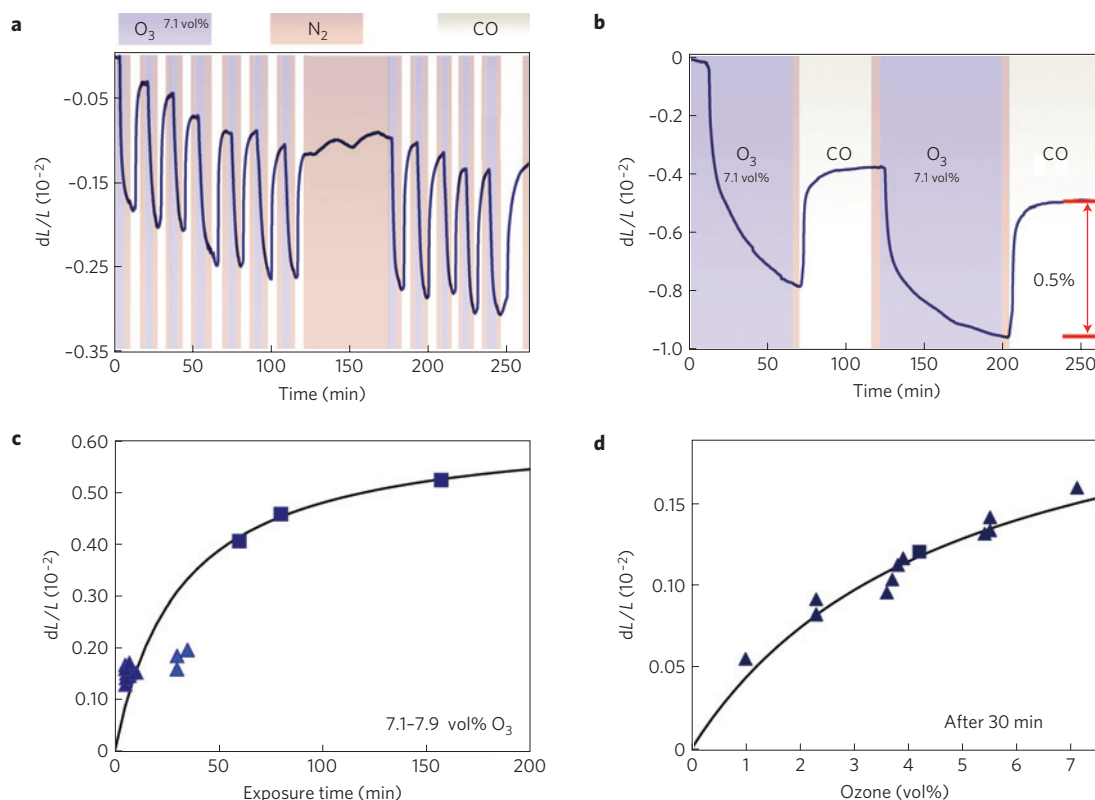
Figure 2 | Performance of a surface-chemistry-driven nanoporous Au actuator. a, Strain versus time as the nanoporous Au actuator is alternately exposed to a mixture of ~7% O_3 in O_2 and pure CO. Between exposures, the sample compartment was purged for 3 min with ultrahigh-purity N_2. Ozone exposure causes contraction, whereas CO exposure restores the original sample dimension. The response is mostly elastic, with only a small irreversible component. The system is very stable, and interrupting the exposure sequence for one hour causes only a small drift of the signal. **b**, Elastic strain amplitudes of up to 0.5% can be realized for long exposures. Note that a strain amplitude of 0.5% corresponds to a macroscopic actuator stroke of 5 µm for a 1-mm-long sample. The irreversible component becomes more pronounced for larger actuator strains. **c**, Elastic strain versus ozone exposure time for a mixture of ~7% O_3 in O_2. **d**, Elastic strain versus ozone concentration for 30 min exposures. Good reproducibility was obtained from different samples (filled squares, filled triangles). The actuator strain increases with both cycle length and O_3 concentration, and typical strain values lie in the range from 0.05 to 0.5%.

nature of our driving reaction. In principle, it should be possible to increase the efficiency by selecting reactions that are accompanied by small entropy and enthalpy changes. Note that the 1 mm cube samples used in the current study contain only ~10^{-6} mol of surface atoms, thus making it a potentially very sensitive sensor material. For example, a miniaturized 10 µm cube could still produce an easy-to-detect 50 nm stroke, which would translate into a detection limit as low as 10^{-12} mol.

The surface stress changes necessary to explain the observed macroscopic dimensional changes can be analysed within a continuum approach. The starting point for such an analysis is the generalized capillary equation for solids[20], which relates the volumetric average of the pressure in the solid to the area average of the surface stress. Assuming that the measured dimensional change $\Delta l/l_o$ is the direct consequence of a surface-stress-induced, linear elastic and isotropic lattice strain, it can be shown that the mean change of surface stress $\langle \Delta f \rangle$ is related to $\Delta l/l_o$ through[7,21]

$$\langle \Delta f \rangle = -\frac{9K}{2\alpha_m \rho} \frac{\Delta l}{l_o}, \qquad (1)$$

where K is the bulk modulus of the solid (220 GPa for Au), α_m is the specific surface area (10–15 $m^2\,g^{-1}$) and ρ is the bulk density (19.3 × 10^6 $g\,m^{-3}$ for Au). According to equation (1), a $\langle \Delta f \rangle$ of 17–26 $N\,m^{-1}$ would be required to explain a compressive strain of 0.005. Although adsorbate-induced changes of f of up

to 15 $N\,m^{-1}$ have been reported for the Cs/Ni(111) system[2], the predicted surface stress change does seem unexpectedly high for oxygen adsorption. In fact, one of the assumptions involved in the derivation of equation (1) must be considered as a poor approximation for nanoporous gold, and the prediction for Δf must thus be viewed as qualitative here. The derivation rests on the assumption that the relative macroscopic volume change of the sample agrees with the volume change of the solid phase, which can be rigorously related to the surface stress change. This is valid when the deformation throughout the porous network can be approximated as an affine stretch. The assumption is plausible for compacts of approximately spherical powder particles of similar size, where it has indeed been confirmed by X-ray diffraction[4]. In contrast, the surface-induced stress in elongated objects—such as the ligaments in nanoporous Au—will typically exhibit a significant shear component[20]. The resulting strain will be non-uniform and locally anisotropic. A continuum mechanics analysis indicates that equation (1) may then overestimate the magnitude of Δf by (in extreme cases) as much as one order of magnitude, in particular for materials with a large Poisson number such as Au (Duan *et al.*, manuscript in preparation). In the absence of a 'calibration', the above results for Δf are therefore qualitative.

Molecular dynamics simulations offer just such an opportunity to independently test the surface stress–strain response of nanoporous Au. Here, we carried out fully atomistic molecular dynamics simulations on the effect of surface stress on the

equilibrium shape of realistic models of nanoporous Au and its structural building blocks, the ligaments. The embedded atom method potential (for more details, see ref. 22) used in this work generates a tensile surface stress of $\sim 1.3\,\mathrm{N\,m^{-1}}$ (at 0 K) for the Au(100) surface, in good agreement with the literature[23]. The skeletal network of our computational nanoporous Au samples was generated by simulating the spinodal decomposition during vapour quenching, and freezing the process once the desired length scale was achieved. The final structure was obtained by adjusting the ligament diameter to produce the desired porosity ($\sim 70\%$), and filling the ligament volume with Au atoms. (100)-oriented Au nanowires were used as models for the ligaments (Fig. 3a). Both samples were created using the atomic positions of bulk face-centred-cubic Au. The effect of tensile surface stress was studied by equilibrating the samples to zero overall pressure at various temperatures ranging from 0 to 300 K. The dimensional changes observed during this relaxation are caused solely by tensile surface stress, and therefore provide a benchmark for the thermodynamic surface stress–strain correlation. An inspection of Fig. 3b reveals that equation (1) indeed underestimates the effect of surface stress: in the case of nanowires, the effect of tensile surface stress is an almost uniaxial contraction along the wire axis ($\Delta L/L \sim \Delta V/V$) and the contraction is approximately seven times larger than predicted by equation (1). The nanoporous samples, on the other hand, show isotropic contraction ($\Delta L/L \sim 1/3\Delta V/V$), and the relaxation is weaker, but still three times stronger than predicted by the thermodynamic approach. The differences between nanowires and nanoporous Au are consistent with the random network structure of the latter, and their lower surface-to-volume ratio. Besides the presence of local shear deformation, the stronger-than-predicted molecular dynamics strain response may also reflect the extremely high fraction of step-edge and kink-site atoms (coordination number 7 and 6, respectively) of these samples. In view of the molecular dynamics results, the experimentally observed strain levels of up to 0.005 can be explained by surface stress changes of $\sim 6\,\mathrm{N\,m^{-1}}$ instead of the $\sim 20\,\mathrm{N\,m^{-1}}$ predicted by the thermodynamic approach.

So far, we have discussed only the size of the adsorbate-induced surface stress changes, but not their sign. Sample contraction (negative strain) as observed on O_3 exposure in the present case (Fig. 2) requires generation of tensile surface stress. Unfortunately, there are still many open questions regarding the atomistic and electronic origin of adsorbate-induced changes of surface stress (for a lucid discussion, see ref. 9).

Qualitatively, however, the behaviour can be understood in terms of a strengthening of the in-plane metal–metal bonds, for example, by depopulation of antibonding metal states through charge transfer from the metal to the adsorbate[24]. For the Au/O system, the accumulation of negative charge on oxygen in the Au/O system is consistent with the higher Pauling electronegativity of O (3.44) with respect to Au (2.54), and has indeed been found in density functional theory calculations[25]. Note, however, that the opposite effect has also been observed. In electrochemical experiments, expansion of nanoporous Au on charge depletion in the surface layer was detected[6], in particular when the potential cycling includes strong OH adsorption/desorption. Such differences may be the result of deviating mechanisms with respect to the stress generation at metal–gas and metal–electrolyte interfaces. Whereas charge-induced changes of the surface stress at solid–electrolyte interfaces seem to be dominated by classical electrostatic interaction of surface atoms with the surface excess charge[26], adsorption on transition-metal surfaces typically involves the formation of localized (covalent) bonds, which directly affects the metal–metal bonding. Nevertheless, a relief of tensile surface stress on oxygen adsorption from the gas phase cannot be generally excluded and has indeed been observed for the Pt(111)/O system[2].
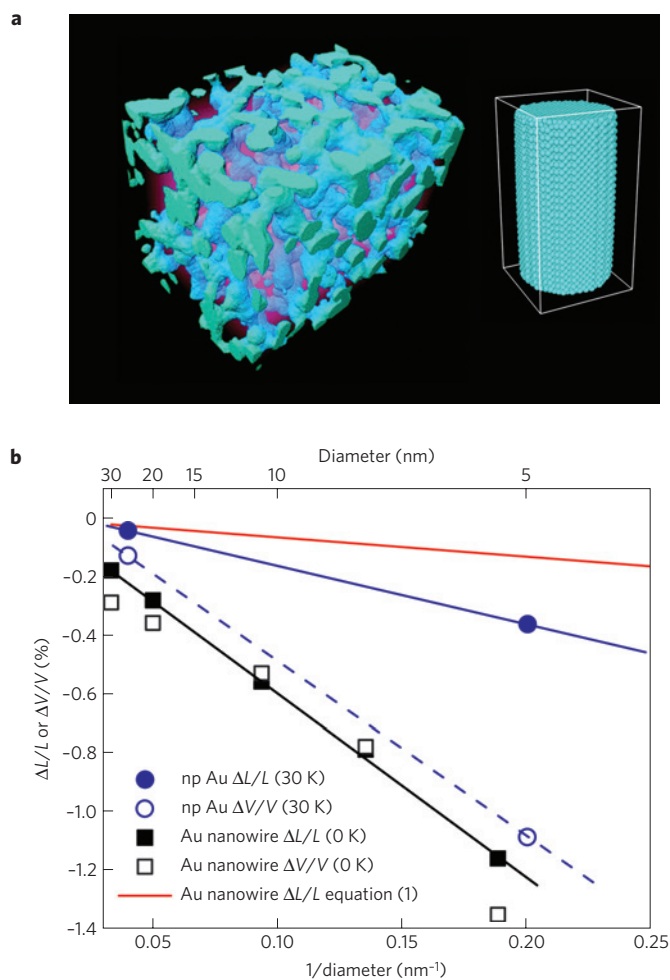
Figure 3 | Surface-stress-induced relaxation of Au nanostructures studied by fully atomistic molecular dynamics simulations.
a, Nanoporous (np) Au and a (100)-oriented Au nanowire resembling the ligaments of nanoporous Au. Nanoporous Au foam samples were generated by simulating the spinodal decomposition during vapour quenching, and freezing the process once the desired length scale was achieved. **b**, Surface-stress-induced relaxation of nanoporous Au and Au nanowire samples during equilibration to zero overall pressure. In the case of nanowires, the effect of tensile surface stress is an almost uniaxial contraction along the wire axis ($\Delta L/L \sim \Delta V/V$) and the contraction is approximately seven times larger than predicted for a locally isotropic deformation (red line). Macroscopic isotropic contraction ($\Delta L/L \sim 1/3\Delta V/V$) is observed for nanoporous Au, consistent with the random network structure of this material.

Beyond charge transfer, adsorbate-induced morphology changes may also have an important role, for example by changing the surface-to-volume ratio. Indeed, oxygen-induced surface roughening through formation of Au-oxide nanoparticles has recently been observed in the Au(111)/O system[27]. To be consistent with our observations, such morphology changes would be required to be reversible. For example, Au atoms released from Au-oxide particles by reaction with CO would be required to heal the defects created by the formation of these Au-oxide particles during O_3 exposure. In this context, the small irreversible strain component observed in our experiments might also be the result of irreversible morphology changes caused by oxygen-enhanced mass transport. Clearly, the origin of the oxygen-induced tensile surface stress generation observed in our experiments is not fully understood yet and will require more detailed studies.

Finally, we want to discuss the role of residual Ag, which is typically of the order of a few at.% for the nanoporous Au samples used in the current study. In principle, residual Ag can affect the O/CO surface chemistry in two ways: first, vacancy formation (atomic scale roughening) by chemically induced dealloying of Ag by adsorbed oxygen and second by increasing the catalytic activity of nanoporous Au. Although the latter effect is important in the context of using nanoporous Au as a low-temperature CO oxidation catalyst that requires the activation of molecular oxygen (O_2), it is not relevant for the current study as we use the more reactive ozone to generate atomically adsorbed oxygen species. Nevertheless, we carried out CO oxidation experiments on Ag-doped nanoporous Au foam samples using the continuous-flow reactor described in ref. 11, which demonstrated that Ag has an important role in the activation of molecular oxygen. The effect of vacancies on surface-stress-induced strain was studied by molecular dynamics simulations on Au nanowires by randomly removing surface atoms. We observed that the presence of surface vacancies weakens the surface-stress-induced strain effect shown in Fig. 3b rather than enhancing it. This result implies that morphological changes including the atomic-scale roughening discussed in the previous paragraph are not the primary cause of the macroscopic strain effect discussed here.

Whether surface-chemistry-driven actuation will develop into an economically viable technology will strongly depend on materials costs, efficiency and long-term stability. The efficiency can be increased by using less energetic reactions than the oxidation of CO by O_3 used here. This will require surface engineering to tailor the surface reactivity, for example by Ag doping to increase the catalytic activity of nanoporous Au towards the dissociation of molecular oxygen, which is a lower-energy fuel. Furthermore, noble-metal-based systems such as nanoporous Au can be replaced by lower-cost, lower-density and stronger high-surface-area materials such as carbon aerogels, for example.

References

1. Ebron, V. H. *et al.* Fuel-powered artificial muscles. *Science* **311**, 1580–1583 (2006).
2. Ibach, H. The role of surface stress in reconstruction, epitaxial growth and stabilization of mesoscopic structures. *Surf. Sci. Rep.* **29**, 193–263 (1997).
3. Baughman, R. H. Playing nature's game with artificial muscles. *Science* **308**, 63–65 (2005).
4. Weissmüller, J. *et al.* Charge-induced reversible strain in a metal. *Science* **300**, 312–315 (2003).
5. Mirfakhrai, T., Madden, J. D. W. & Baughman, R. H. Polymer artificial muscles. *Mater. Today* **10**, 30–38 (2007).
6. Kramer, D., Viswanath, R. N. & Weissmüller, J. Surface-stress induced macroscopic bending of nanoporous gold cantilevers. *Nano Lett.* **4**, 793–796 (2004).
7. Viswanath, R. N., Kramer, D. & Weissmüller, J. Adsorbate effects on the surface stress-charge response of platinum electrodes. *Electrochim. Acta* **53**, 2757–2767 (2008).
8. Haiss, W. Surface stress of clean and adsorbate-covered solids. *Rep. Prog. Phys.* **64**, 591–648 (2001).
9. Feibelman, P. J. First-principles calculations of stress induced by gas adsorption on Pt(111). *Phys. Rev. B* **56**, 2175–2182 (1997).
10. Kim, J., Samano, E. & Koel, B. E. Oxygen adsorption and oxidation reactions on Au(211) surfaces: Exposures using O_2 at high pressures and ozone (O_3) in UHV. *Surf. Sci.* **600**, 4622–4632 (2006).
11. Zielasek, V. *et al.* Gold catalysts: Nanoporous gold foams. *Angew. Chem. Int. Ed.* **45**, 8241–8244 (2006).
12. Biener, M. M., Biener, J. & Friend, C. M. Enhanced transient reactivity of an O-sputtered Au(111) surface. *Surf. Sci.* **590**, L259–L265 (2005).
13. Erlebacher, J. *et al.* Evolution of nanoporosity in dealloying. *Nature* **410**, 450–453 (2001).
14. Biener, J. *et al.* Size effects on the mechanical behavior of nanoporous Au. *Nano Lett.* **6**, 2379–2382 (2006).
15. van Bokhoven, J. A. *et al.* Activation of oxygen on gold/alumina catalysts: *In situ* high-energy-resolution fluorescence and time-resolved X-ray spectroscopy. *Angew. Chem. Int. Ed.* **45**, 4651–4654 (2006).
16. Newman, R. C. *et al.* Alloy corrosion. *MRS Bull.* **24**, 24–28 (1999).
17. Cattarin, S., Kramer, D., Lui, A. & Musiani, M. M. Preparation and characterization of gold nanostructures of controlled dimension by electrochemical techniques. *J. Phys. Chem. C* **111**, 12643–12649 (2007).
18. Yim, W. L. *et al.* Universal phenomena of CO adsorption on gold surfaces with low-coordinated sites. *J. Phys. Chem. C* **111**, 445–451 (2007).
19. Hodge, A. M. *et al.* Scaling equation for yield strength of nanoporous open-cell foams. *Acta Mater.* **55**, 1343–1349 (2007).
20. Weissmüller, J. & Cahn, J. W. Mean stresses in microstructures due to interface stresses: A generalization of a capillary equation for solids. *Acta Mater.* **45**, 1899–1906 (1997).
21. Viswanath, R. N., Kramer, D. & Weissmüller, J. Variation of the surface stress-charge coefficient of platinum with electrolyte concentration. *Langmuir* **21**, 4604–4609 (2005).
22. Zepeda-Ruiz, L. A. *et al.* Mechanical response of freestanding Au nanopillars under compression. *Appl. Phys. Lett.* **91**, 101907 (2007).
23. Diao, J. K., Gall, K. & Dunn, M. L. Atomistic simulation of the structure and elastic properties of gold nanowires. *J. Mech. Phys. Solids* **52**, 1935–1962 (2004).
24. Fiorentini, V., Methfessel, M. & Scheffler, M. Reconstruction mechanism of fcc transition-metal (001) surfaces. *Phys. Rev. Lett.* **71**, 1051–1054 (1993).
25. Torres, D., Neyman, K. M. & Illas, F. Oxygen atoms on the (111) surface of coinage metals: On the chemical state of the adsorbate. *Chem. Phys. Lett.* **429**, 86–90 (2006).
26. Umeno, Y. *et al.* Ab initio study of surface stress response to charging. *EPL* **78**, 13001 (2007).
27. Min, B. K. *et al.* Efficient CO oxidation at low temperature on Au(111). *J. Phys. Chem. B* **110**, 19833–19838 (2006).

Additional information

Reprints and permissions information is available online at http://npg.nature.com/reprintsandpermissions. Correspondence and requests for materials should be addressed to J.B.